

Supporting Information

Nanocubic Copper Doped SrTiO₃ for Photoreduction of Cr (VI) and Photodegradation of Methyl Violet

Uma P.I.^a, U. Sandhya Shenoy^{b,*}, D. Krishna Bhat^{a,*}

^aDepartment of Chemistry, National Institute of Technology Karnataka, Surathkal,
Mangalore 575025, India

^bDepartment of Materials Science and Engineering, Institute of Engineering and Technology,
Srinivas University, Mukka, Mangalore 574146, India

*Corresponding authors: denthajekb@gmail.com; sandhyashenoy347@gmail.com

Methods

S1. Synthesis

All the chemicals purchased from Sigma Aldrich were directly used without purification. 1.5 mL of titanium isopropoxide was dissolved in 10 mL of isopropanol. To this calculated amount of copper acetate and strontium nitrate were added and magnetically stirred for 30 minutes to attain complete dissolution. About 15 mL 5 M KOH solution was added dropwise. After the addition, the mixture was allowed to stir for 1 hour. The resultant mixture was sealed in an autoclave and kept in a hot air oven maintained at 200 °C for 4 hours. The obtained mixture was neutralized with acetic acid to pH 7 and washed with distilled water to remove the impurities present. Then the product was dried in an oven at 50 °C overnight.

S2. Characterisation

To determine the phase and purity of the prepared materials, we utilized an X-ray diffractometer (XRD, Rigaku Miniflex 600) set up with monochromatic Cu K radiation ($\lambda = 0.154$ nm) at a scan rate of 2° per minute in the 2 θ range of 20°-80°. Using transmission electron microscopy (TEM, FEI Tecnai G2 Spirit Bio- Twin TEM 120kV) and field emission scanning electron microscopy (FESEM, Joel 7610FPLUS) the surface morphology and structure of the produced materials were examined. The elemental analysis of the samples was carried out using energy dispersive X-ray (EDX) spectroscopy (Oxford INCA EDS 140 eV). An Al K source equipped Thermofisher Scientific Nexsa base spectrometer was utilised to capture the X-ray photoelectron spectrum (XPS). Using the Brunauer-Emmett-Teller (BET) method, we calculated the precise surface area, pore volume and pore size distribution (Autosorb IQ-XR-XR, Anton Paar, Austria). A UV-visible spectrometer was used to get the diffuse reflectance (DR) spectrum data (Perkin Elmer LAMBDA 950). At room temperature, the photoluminescence (PL) spectra were captured using Fluoromax-4 Spectrofluorometer.

S3. Determination of photoreduction activity

A broadband ceramic discharge metal halide lamp (Philips MASTER Colour CDM-R/830) with a doped tungsten electrode was used for measuring the photocatalytic activity as a visible light source. The catalyst (40 mg) was dissolved in 50 mL of potassium dichromate solution at a concentration of around 100 mg L⁻¹. About 1 g of fructose was added to the mixture, and the appropriate volume of 0.5 M H₂SO₄ was employed to bring the pH of the mixture down to an acidic level (<5).^{1,2} To achieve equal dispersion, sonication was carried out for 10 minutes. The dish was then inserted into the reactor with a magnetic stirrer and the light

source was turned on. About 5 mL of the solution was taken out at 5 minutes intervals to monitor the reduction process. After centrifuging to remove the catalyst, the solution was spectrophotometrically analysed to find the absorbance and eventually the concentration at specific intervals. With the use of a UV-visible spectrometer calibrated to 350 nm for potassium dichromate, the absorbance of the supernatant solution was calculated. The percentage of reduction was calculated by equation (1):

$$\text{Reduction \%} = [(C_0 - C)/C_0] \times 100 \quad (1)$$

where C_0 is the initial concentration of the potassium dichromate solution and C is the concentration at different intervals of time.

S4. Determination of photocatalytic activity

About 100 mL of methyl violet (MV) solution (10 mg L^{-1}) and 50 mg of the catalyst were taken in a crystallizing dish and sonicated for 10 minutes for uniform dispersion. The light source was turned on once the dish was put into the reactor. About 5 mL of the solution was sampled at intervals of 30 minutes and evaluated spectrophotometrically. The absorbance of the supernatant dye solution was measured using a UV-visible spectrophotometer calibrated to 587 nm for methyl violet. The percentage of degradation was calculated by same method using the equation above where C_0 is the initial concentration of the dye solution and C is the concentration at different intervals of time.^{3,4}

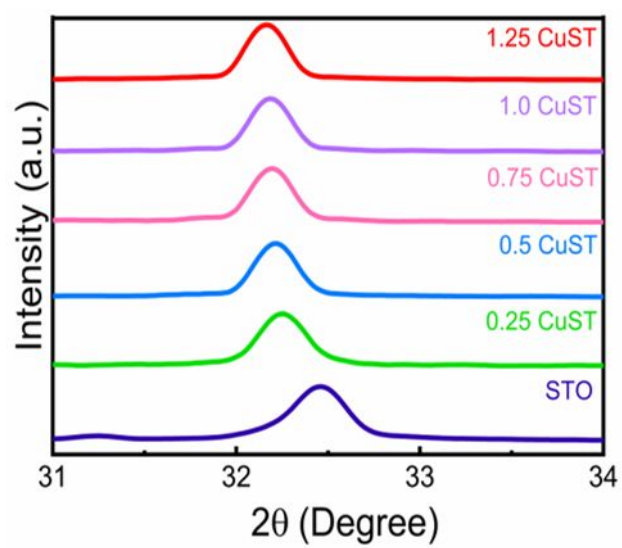


Fig. S1. XRD patterns of SrTiO₃ and Cu doped SrTiO₃ with varying concentrations of Cu.

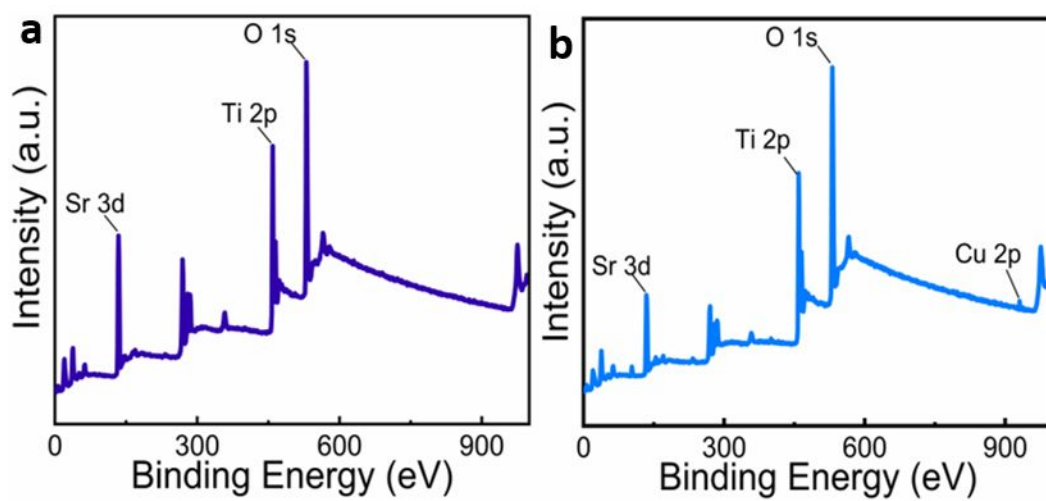


Fig. S2. XPS survey spectra of (a) SrTiO₃ and (b) Cu doped SrTiO₃ nanocubes.

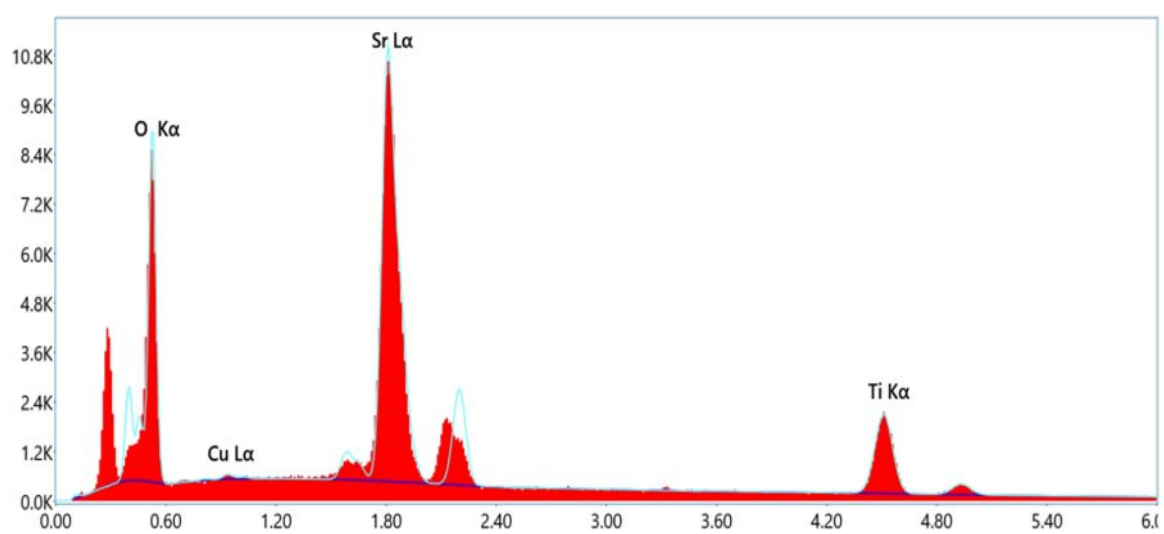


Fig. S3. EDX spectrum of Cu doped SrTiO₃ nanocubes.

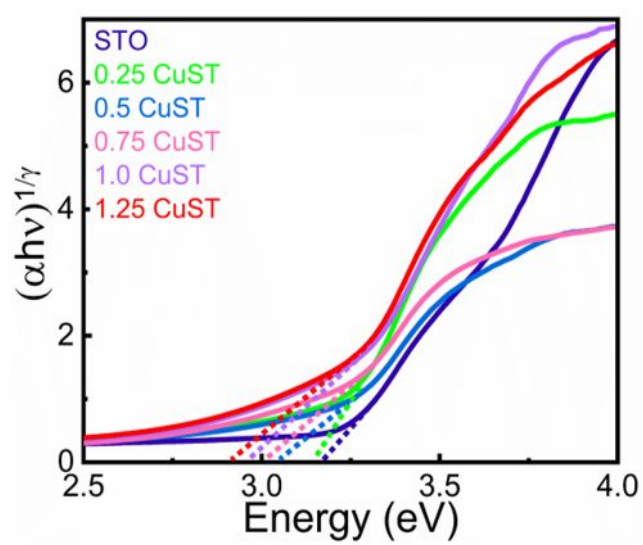


Fig. S4. Tauc plot of SrTiO₃ and Cu doped SrTiO₃.

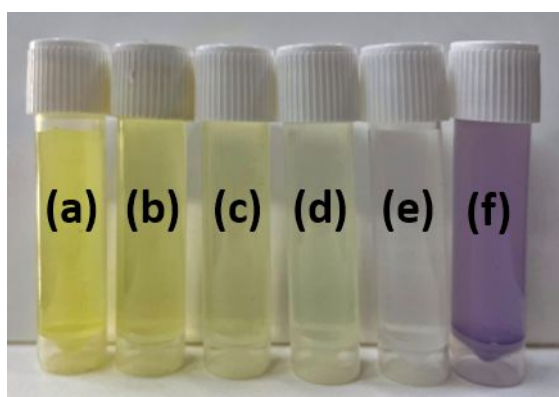


Fig. S5. Colour change during the photoreduction of potassium dichromate at (a) 0, (b) 5, (c) 15, (d) 25 and (e) 35 minutes, (f) after complexation with EDTA.

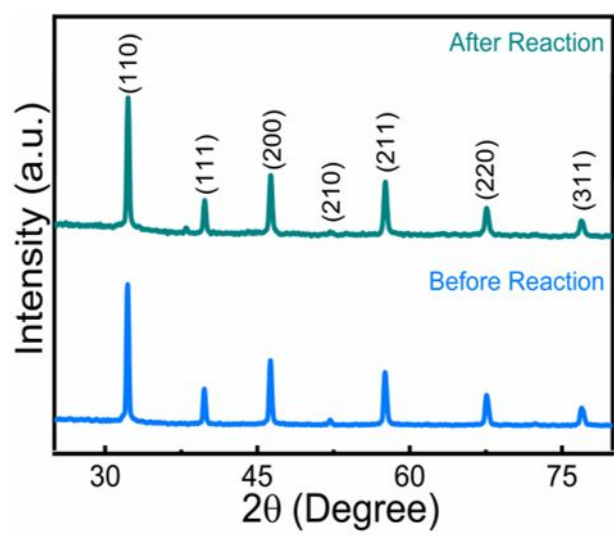


Fig. S6. XRD patterns of 0.5 CuST before and after photocatalytic reaction.

Table S1. Thermodynamic parameters of SrTiO₃ and Cu doped SrTiO₃ samples for photoreduction of Cr⁶⁺.

Samples	E _a (kJ mol ⁻¹)	ΔH [#] (kJ mol ⁻¹)	ΔS [#] (kJ mol ⁻¹)	ΔG [#] (kJ mol ⁻¹)
Blank	9.6	7.1	-0.25	83.1
STO	8.4	5.9	-0.25	81.8
0.25 CuST	5.7	3.3	-0.25	79.2
0.5 CuST	3.2	0.7	-0.25	76.7
0.75 CuST	5.4	2.9	-0.25	78.9
1.0 CuST	5.8	3.3	-0.25	79.3
1.25 CuST	5.8	3.3	-0.25	79.3

The Eyring equation and the activation complex theory (ACT) were used to compute the energy of activation (E_a), the free energy of activation (ΔG[#]), the enthalpy of activation (ΔH[#]) and the entropy of activation (ΔS[#]).⁵ Table S1 provides information on the thermodynamics of Cr⁶⁺ reduction. The reaction had the lowest activation energy, activation enthalpy, and activation free energy in presence of 0.5 CuST sample as catalyst as expected resulting in high rate of reaction.

Table S2. Thermodynamic parameters of SrTiO₃ and Cu doped SrTiO₃ samples for photocatalytic degradation of MV dye.

Samples	E _a (kJ mol ⁻¹)	ΔH [#] (kJ mol ⁻¹)	ΔS [#] (kJ mol ⁻¹)	ΔG [#] (kJ mol ⁻¹)
Blank	14.6	12.1	-0.25	88.1
STO	11.2	8.7	-0.25	84.7
0.25 CuST	9.2	6.7	-0.25	82.6
0.5 CuST	8.0	5.8	-0.25	81.5
0.75 CuST	8.5	6.0	-0.25	82.0
1.0 CuST	8.8	6.3	-0.25	82.3
1.25 CuST	9.0	6.5	-0.25	82.4

Table S3. Comparison of photocatalytic efficiency of 0.5 CuST sample with reported works of literature.

Photocatalyst	Light source	Pollutant (Initial concentration in mg L ⁻¹)	Degradation extent and time in min	Reference
Cu doped SrTiO ₃	Visible (Philips MASTER Colour CDM-R/830)	Cr ⁶⁺ (100)	99 %, 15 100 %, 25	Present work
		MV dye (10)	99 %, 120	
Cu doped BaTiO ₃	Visible (Philips MASTER Colour CDM-R/830)	Cr ⁶⁺ (100)	99.8 %, 20	Uma et al., 2023 [6]
		MV dye (10)	99.4 %, 120	
N doped SrTiO ₃	300W Mercury Lamp	Cr ⁶⁺ (5)	69 %, 130	Xing et al., 2016 [7]
Nb doped SrTiO ₃	Xenon Lamp	Cr ⁶⁺ (20)	100 %, 75	Zhu et al., 2022 [8]
SrTiO ₃	500 W Xenon Arc Lamp	Cr ⁶⁺ (10)	100 %, 120	Yang et al., 2016 [9]
Ce doped BaTiO ₃	UV (254 nm) and Visible (400-750 nm, 300 W Tungsten-Halogen Lamp)	MV dye (5)	82.4 %, 120	Senthilkumar et al., 2019 [10]
Graphite/PbTiO ₃ Composite	9 W UV Lamp	MV dye (5)	92.2 %, 30	Purnawan et al., 2018 [11]

References

1. Yi, X. H.; Ma, S. Q.; Du, X. D.; Zhao, C.; Fu, H.; Wang, P.; Wang, C. C.; Velegraki, G.; Miao, J.; Drivas, C.; Liu, B.; Kennou, S.; Armatas, G. S. The Facile Fabrication of 2D/3D Z-Scheme g-C₃N₄/UiO-66 Heterojunction with Enhanced Photocatalytic Cr(VI) Reduction Performance under White Light. *Appl. Catal. B Environ.* **2018**, *375*, 635–644.
2. Yan, B.; Chen, Z. Influence of pH on Cr(VI) Reduction by Organic Reducing Substances from Sugarcane Molasses. *Appl. Water Sci.* **2019**, *9*, 1–8.
3. Bhat, D. K.; Bantawal, H.; Shenoy, U. S. Rhodium Doping Augments Photocatalytic Activity of Barium Titanate: Effect of Electronic Structure Engineering. *Nanoscale Adv.* **2020**, *2*, 5688–5698.
4. Sadiq, M. M. J.; Shenoy, U. S.; Bhat, D. K. Enhanced Photocatalytic Performance of N-Doped RGO-FeWO₄/Fe₃O₄ Ternary Nanocomposite in Environmental Applications. *Mater. Today Chem.* **2017**, *4*, 133–141.
5. Bantawal, H.; Shenoy, U. S.; Bhat, D. K. Vanadium-Doped SrTiO₃ Nanocubes: Insight into Role of Vanadium in Improving the Photocatalytic Activity. *Appl. Surf. Sci.* **2020**, *513*, 145858.
6. Uma, P. I.; Shenoy, U. S.; Bhat, D. K. Electronic Structure Engineering of BaTiO₃ Cuboctahedrons by Doping Copper to Enhance the Photocatalytic Activity for Environmental Remediation. *J. Alloys Compd.* **2023**, *948*, 169600.
7. Xing, G.; Zhao, L.; Sun, T.; Su, Y.; Wang, X. Hydrothermal Derived Nitrogen Doped SrTiO₃ for Efficient Visible Light Driven Photocatalytic Reduction of Chromium(VI). *Springerplus* **2016**, *5*, 1-13.
8. Zhu, J.; Zhang, Y. Y.; Shen, L.; Li, J.; Li, L.; Zhang, F.; Zhang, Y. Y. Hydrothermal Synthesis of Nb⁵⁺-Doped SrTiO₃ Mesoporous Nanospheres with Greater Photocatalytic Efficiency for Cr(VI) Reduction. *Powder Technol.* **2022**, *410*, 117886.
9. Yang, D.; Sun, Y.; Tong, Z.; Nan, Y.; Jiang, Z. Fabrication of Bimodal-Pore SrTiO₃ Microspheres with Excellent Photocatalytic Performance for Cr(VI) Reduction under Simulated Sunlight. *J. Hazard. Mater.* **2016**, *312*, 45–54.
10. Senthilkumar, P.; Jency, D. A.; Kavinkumar, T.; Dhayanithi, D.; Dhanuskodi, S.; Umadevi, M.; Manivannan, S.; Giridharan, N. V.; Thiagarajan, V.; Sriramkumar, M.; Jothivenkatachalam, K. Built-in Electric Field Assisted Photocatalytic Dye Degradation and Photoelectrochemical Water Splitting of Ferroelectric Ce Doped BaTiO₃ Nanoassemblies. *ACS Sustain. Chem. Eng.* **2019**, *7*, 12032–12043.
11. Purnawan, C.; Wahyuningsih, S.; Nawakusuma, V. Methyl Violet Degradation Using

Photocatalytic and Photoelectrocatalytic Processes over Graphite/PbTiO₃ Composite.
Bull. Chem. React. **2018**, *13*, 127–135.